Available online at www.sciencedirect.com

SCIENCE DIRECT®

Biochimica et Biophysica Acta 1659 (2004) 19–31

BIOCHIMICA ET BIOPHYSICA ACTA
BBA

http://www.elsevier.com/locate/bba

Molecular interference of Cd^{2+} with Photosystem II

Kajsa G.V. Sigfridsson[1,2], Gábor Bernát[2,3], Fikret Mamedov[1], Stenbjörn Styring[1,*]

Department of Biochemistry, Center for Chemistry and Chemical Engineering, Lund University, P.O. Box 124, S-221 00 Lund, Sweden

Received 26 April 2004; received in revised form 23 June 2004; accepted 7 July 2004
Available online 2 August 2004

Abstract

Many heavy metals inhibit electron transfer reactions in Photosystem II (PSII). Cd^{2+} is known to exchange, with high affinity in a slow reaction, for the Ca^{2+} cofactor in the Ca/Mn cluster that constitutes the oxygen-evolving center. This results in inhibition of photosynthetic oxygen evolution. There are also indications that Cd^{2+} binds to other sites in PSII, potentially to proton channels in analogy to heavy metal binding in photosynthetic reaction centers from purple bacteria. In search for the effects of Cd^{2+}-binding to those sites, we have studied how Cd^{2+} affects electron transfer reactions in PSII after short incubation times and in sites, which interact with Cd^{2+} with low affinity. Overall electron transfer and partial electron transfer were studied by a combination of EPR spectroscopy of individual redox components, flash-induced variable fluorescence and steady state oxygen evolution measurements. Several effects of Cd^{2+} were observed: (i) the amplitude of the flash-induced variable fluorescence was lost indicating that electron transfer from Y_Z to P_{680}^+ was inhibited; (ii) Q_A^- to Q_B electron transfer was slowed down; (iii) the S_2 state multiline EPR signal was not observable; (iv) steady state oxygen evolution was inhibited in both a high-affinity and a low-affinity site; (v) the spectral shape of the EPR signal from $Q_A^-Fe^{2+}$ was modified but its amplitude was not sensitive to the presence of Cd^{2+}. In addition, the presence of both Ca^{2+} and DCMU abolished Cd^{2+}-induced effects partially and in different sites. The number of sites for Cd^{2+} binding and the possible nature of these sites are discussed.

Keywords: Cadmium; Calcium; DCMU; EPR; Fluorescence; Photosystem II

1. Introduction

Photosystem II (PSII) is a large enzyme complex situated in the thylakoid membrane in plants, algae and cyanobacteria [1,2]. It catalyzes the light-driven reduction of plastoquinone using electrons extracted from water by the OEC. The three-dimensional structure of PSII in thermophilic cyanobacteria was first determined at 3.8- and 3.7-Å resolutions [3,4] and more recently at 3.5-Å resolution [5]. The structures have revealed the transmembrane helical structure, the backbone tracing of core proteins, the position of the chlorophylls and carotenoids in the core antenna and also detailed pictures of the redox cofactors in PSII. The 3.5-Å structure [5] also allowed positioning of most of the amino acid side chains. The Ca/Mn cluster that catalyzes water oxidation is situated ~20 Å from the primary donor P_{680} and ~7–8 Å from the intermediary electron donor Y_Z. The cluster contains four Mn ions and the recent X-ray data [5] also allowed positioning of the Ca^{2+} ion directly in the

Abbreviations: Chl, chlorophyll; Cyt, cytochrome; DCMU, 3-(3′,4′-dichlorophenyl)-1,1-dimethylurea; EPR, electron paramagnetic resonance; F_{max}, the maximal fluorescence from Q_A^-; F_0, initial fluorescence before the actinic flash; F_v, variable fluorescence $F_{max}-F_0$; MES, 4-morpholineethanesulfonic acid; ML, multiline EPR signal in S_2 state; OEC, oxygen evolving complex; P*p*BQ, phenyl-*p*-benzoquinone; PSII, Photosystem II; P_{680}, primary donor of PSII; Q_A and Q_B, the primary and secondary quinone acceptors in PSII; S-states, $S_0 \rightarrow S_4$ are the different redox states of the Ca/Mn cluster; Y_Z and Y_D, redox-active tyrosine residues D1-161 and D2-160 in PSII

* Corresponding author. Tel.: +46 18 471 65 80; fax: +46 18 55 98 85.
E-mail address: stenbjorn.styring@biokem.lu.se (S. Styring).
[1] Current address: Molecular Biomimetics, Uppsala University, Villavägen 6, S-752 36 Uppsala, Sweden.
[2] These authors equally contributed to this paper.
[3] Current address: Leibniz-Institute for Neurobiology, Special Lab Non-Invasive Brain Imaging, Brenneckestrasse 6, D-39118 Magdeburg, Germany.

0005-2728/$ - see front matter © 2004 Elsevier B.V. All rights reserved.
doi:10.1016/j.bbabio.2004.07.003

Mn core of the catalytic unity. Ca^{2+} is a cofactor for water oxidation, which has been much studied. Correctly, it was long considered to bind very close to the four Mn ions (within 3–4 Å [6–8]) but the first structures did not resolve this issue, which led to much speculation in the field. The knowledge gained from the structure of how Ca^{2+} and four Mn ions together form a dense cluster connected by bridging oxygens and common carboxylates from identified side chains [5] resolves many issues but also brings new detailed questions to be addressed.

An interesting feature in the X-ray data is the presence of a bound Cd^{2+} ion that originates from the heavy metal derivative used to resolve the phase of the X-ray diffraction pattern in the determination of the crystal structure [3,9]. The Cd^{2+} ion is bound at the internal end of an extended β-barrel structure in the 33-kDa PsbO protein that covers the Ca/Mn cluster. The distance between the Cd^{2+} ion and the Ca/Mn cluster is 30–40 Å. The presence of this Cd^{2+} ion prompted Rutherford and Faller [9] to speculate that it binds in the site normally occupied by the Ca^{2+} cofactor. This speculation was not correct, but as pointed out, the position of this Cd^{2+} ion is interesting in itself since Cd^{2+} is known to inhibit photosynthetic electron transfer in reaction centers from purple bacteria and PSII (see below).

Cd^{2+} inhibition of overall (oxygenic) photosynthesis or partial reactions in bacterial photosynthetic reaction centers or PSII has been studied by several groups [10–24]. Recently, it was shown that Cd^{2+} binds with a binding constant of 100–200 μM, thereby inhibiting steady state oxygen evolution in a PSII enriched membrane preparation [22]. The Cd^{2+} ion was in competition for this site with Ca^{2+} and it was consequently concluded that the Cd^{2+} binding site is located on the donor side of PSII. The same conclusion was drawn from solid-state ^{113}Cd-NMR experiments [20]. Cd^{2+} was also found to compete efficiently with Ca^{2+} during photoactivation of Mn-depleted PSII (Peter Faller, personal communication). It was concluded that the intact Ca/Mn cluster has a higher selectivity for Ca^{2+} over Cd^{2+} than Mn-depleted PSII during photoactivation. This makes sense as the structure reveals that Ca^{2+} actually is an integral part of the Ca/Mn cluster [5] and it seems that Cd^{2+} might actually exchange for Ca^{2+} in the site. This seemingly is a very slow process, which takes several hours to reach equilibrium [22].

In contrast to the known binding of Ca^{2+} to the donor side of PSII, a Cd^{2+} binding site was found at the acceptor side in bacterial reaction centers [17,19,24]. Binding of Cd^{2+} to His-126 and His-128 in the H-subunit of reaction centers from *Rb. sphaeroides* slows down the Q_B^- protonation rate by blocking the proton channel to the Q_B site. This led to a speculation that the Cd^{2+} observed in the X-ray work (see above) might actually block a similar proton channel in or close to the 33-kDa PsbO protein, this time involved in proton release from the OEC in oxygenic organisms [9].

Many heavy metal ions inhibit the oxygen evolution and electron transfer through PSII. In most cases, the inhibitory sites have not been conclusively determined but, in some cases, for example Cu^{2+}, the applied methods have allowed more precise identification [22,25–32]. It has been shown by fluorescence and EPR analysis [29] that addition of Cu^{2+} inhibits PSII electron transfer at sites on both the donor and acceptor side. The acceptor-side effect of Cu^{2+} was revealed as a magnetic decoupling of the acceptor-side Fe^{2+} and Q_A^- resulting in a free radical EPR signal from Q_A^- [29]. On the donor side, Cu^{2+} inhibited the electron transfer between Y_Z and P_{680} [29]. In addition Cu^{2+} [29] and different lanthanides [33] have been found to remove extrinsic subunits (Cu^{2+} removed the 17-kDa; La^{3+} removed both the 17- and 23-kDa) from the OEC.

The existence of two (or more) binding sites with different inhibitory function might also be relevant for Cd^{2+}. However, there are no data available to support this and all studies on Cd^{2+} inhibition of PSII have been directed towards the binding of Cd^{2+} in the Ca^{2+} site, which is now known to be directly in the Ca/Mn cluster [5]. The Cd^{2+} binding has mainly been analyzed through inhibition of overall electron transfer through PSII, assayed for example by the oxygen evolution [10,12,13,22]. In the present study, we use more resolving techniques, EPR spectroscopy and flash-induced variable fluorescence, to follow the effect of Cd^{2+} on individual redox components and partial reactions in PSII (in addition to the oxygen evolution). Our results indicate that there are at least three modes of action of Cd^{2+} in PSII.

2. Materials and methods

2.1. PSII membrane preparation

PSII-enriched membrane fragments (BBY particles) were prepared from greenhouse grown spinach (*Spinacia oleracea*) according to Ref. [34] with modifications as in Ref. [35]. The BBY particles were suspended in a buffer containing 10 mM $MgCl_2$, 10 mM NaCl, 5 mM $CaCl_2$, 400 mM sucrose and 20 mM MES–NaOH pH 6.0 and stored at 10 mg Chl ml^{-1} at −80 °C until use. Chl determinations were made according to Arnon [36]. Salt washing of the PSII enriched membranes to remove the extrinsic 23- and 17-kDa proteins was done by standard procedures involving incubation with 1 M NaCl for 30 min on ice [37]. Complete removal of the subunits was ensured by SDS-PAGE analysis.

2.2. PSII activity measurements

Steady state oxygen evolution at 20 °C was measured with a Clark-type electrode (Hansatech Instruments, UK). The Chl concentration was 10 μg Chl ml^{-1}. P*p*BQ (0.5 mM) was used as electron acceptor. The measuring buffer contained 10 mM

$MgCl_2$, 15 mM NaCl, 400 mM sucrose and 20 mM MES-NaOH pH 6.0. In the control samples, the rate of the oxygen evolution was 400–450 μmol oxygen (mg Chl)$^{-1}$ h^{-1}, which is normal for this type of preparation from spinach growing under our cultivation protocol. In the salt-washed membranes, the oxygen evolution, measured in the presence of 10 mM $CaCl_2$, was ca 320 μmol oxygen (mg Chl)$^{-1}$ h^{-1}.

In Cd^{2+} inhibition experiments, the PSII membranes (at 10 μg Chl ml^{-1}) were incubated with 0–10 mM $CdCl_2$ for 5 min at room temperature. Five-minute incubation was chosen since our objective was to elucidate if there existed early Cd^{2+} effects in sites different from the Ca^{2+} site where the exchange is known to be slow [22] (see Results). Similar experiments were made with $CaCl_2$ (0–10 mM). To study the competition between Cd^{2+} and Ca^{2+}, Cd^{2+} incubation experiments as described above were repeated in the presence of $CaCl_2$. The applied Ca^{2+} concentrations were 0.8, 1.5, 3.0 and 5.0 mM, respectively.

The reversibility of the Cd^{2+} inactivation was tested in an experiment where the PSII particles, at 50 μg Chl ml^{-1}, were incubated with Cd^{2+} (0 or 2 mM) prior to a washing procedure. During Cd^{2+} inhibition, the samples were suspended in a buffer containing 10 mM $MgCl_2$, 15 mM NaCl, 400 mM sucrose and 20 mM MES–NaOH pH 6.0. After 5 min, the samples were centrifuged for 20 min at 27 000×g. The pellets were resuspended in the same buffer to 1 mg Chl ml^{-1}. For comparison to the washed samples, parallel samples incubated in the same manner, but not washed, were prepared (further referred to as "unwashed"). The samples were measured with or without the addition of 5 mM $CaCl_2$ (5-min incubation was applied before the measurement).

2.3. Flash-induced variable fluorescence measurements

Flash-induced variable fluorescence was measured with a double modulated FL-100 fluorimeter (Photon System Instruments, Brno, Czech Republic). The saturating actinic flash duration was 50 μs. The first data point was collected 100 μs after the actinic flash. Four data points per decade in the logarithmic time scale were acquired by applying measuring light pulses (2.5-μs duration). The measuring time was 60 s. The actinic flash and the measuring light pulses were provided by red light-emitting diodes. The data were collected with the FluorWin software (Photon System Instruments).

The fluorescence experiments were performed in dark-adapted PSII membranes at 10 μg Chl ml^{-1}, incubated for 5 min with 0–10 mM Cd^{2+}. Competition between Ca^{2+} and Cd^{2+} was investigated by a similar experiment carried out in the presence of 5 mM $CaCl_2$. To improve the signal to noise ratio, nine traces at each Cd^{2+} and/or Ca^{2+} concentration were averaged. These nine traces were recorded in three samples and each sample was measured three times. The time between each measurement was 3 min to allow relaxation of the sample prior to the next measurement. The maximal fluorescence level, F_{max}, was determined in the presence of 17 mM dithionite.

The flash-induced fluorescence in presence of DCMU was measured with a PAM-100 fluorimeter (Walz, Effeltrich, Germany) according to Ref. [38]. Dark-adapted PSII samples at 20 μg Chl ml^{-1} were incubated for 5 min in a Cd^{2+} (0–10 mM)- and DCMU (20 μM)-containing buffer. Single measurements from 10 independent samples were averaged to obtain the fluorescence decay traces that were analysed for fluorescence amplitude and decay kinetics.

The analysis of the fluorescence decay kinetics was done by multi-exponential fitting according to

$$F(t) - F_0 = A_1 e^{-k_1 t} + A_2 e^{-k_2 t} + A_3 e^{-k_3 t} \quad (1)$$

where $F(t)$ is the fluorescence value at time t, A_n is the amplitude and k_n is the rate constant of the different decay phases and F_0 is the initial fluorescence before the actinic flash.

2.4. EPR spectroscopy

Low-temperature EPR measurements were performed with a Bruker ELEXYS500E spectrometer using a SuperX EPR049 microwave bridge and an ER4122SHQ cavity. The system was fitted with an Oxford instruments, UK cryostat and temperature controller.

For EPR experiments, the PSII enriched membranes were diluted to ca 4 mg Chl ml^{-1}. To oxidize Y_D completely (providing the stable $Y_D^{\bullet}$ radical in all PSII centers) the samples were pre-illuminated for 3 min at 20 °C using room-light followed by a 15-min dark incubation to allow relaxation of higher S-states. After the pre-illumination and subsequent dark incubation, Cd^{2+}, Ca^{2+}, or DCMU was added in the dark. After 5-min incubation, the samples were frozen and EPR spectra were recorded. The EPR samples were 2–300 times more concentrated than the samples used for oxygen evolution and fluorescence experiments. Therefore, we used the 10–100 mM $CdCl_2$ concentration range in the EPR experiments. This makes direct comparison of binding parameters very difficult between the EPR experiments and the activity measurements (oxygen evolution and variable fluorescence). In competition experiments, 25 mM Ca^{2+} or 1 mM DCMU and varying Cd^{2+} concentrations were added in one addition.

The EPR signal from $Y_D^{\bullet}$ was used as an internal standard. At normal pH, $Y_D^{\bullet}$ is very stable and after our pre-illumination and dark-adaptation procedure, it is safe to assume that $Y_D^{\bullet}$ amounts to one radical per PSII center [39,40].

In many cases, the EPR spectra were recorded directly on the dark-adapted samples and after continuous, strong white light illumination for 10 min at 200 K in a dry ice ethanol bath. Illumination at 200 K allows one stable charge separation in PSII (at 200 K electron transfer between Q_A and Q_B is blocked [41,42]), which permits studies of the S_1

to S_2 transition, of Q_A^- and of the function of accessory donors in PSII.

3. Results

3.1. Incubation time with Cd^{2+}

We have chosen a short incubation time with Cd^{2+} since our intention was to investigate early inhibition phases, keeping the option of several Cd^{2+} sites in mind. Five-minute incubation time was determined to be optimal for our purpose from an experiment, where the inhibition of oxygen evolution after incubation with 2 mM $CdCl_2$, for different times up to 20 min, was followed (not shown). During the first 2–3 min of Cd^{2+} incubation, the activity declined rapidly and ca 20% of the oxygen evolution was lost. Thereafter the activity levelled off and after 5-min incubation the inhibition was only slightly above 20%. Continued incubation with Cd^{2+} led to a slow steady decrease of the oxygen evolution. After 10-, 15- and 20-min incubation, the inhibition was 25%, 30% and 40%, respectively. The control (no added Cd^{2+}) was only inhibited by 4% after 15-min incubation. From these results we decided to incubate PSII with Cd^{2+} for 5 min to investigate the "fast effect" in detail. In essence, our results agree with those in Ref. [22] where it was concluded that it took several hours to reach complete equilibrium with Cd^{2+} in inhibition of oxygen evolution.

3.2. Inhibition of steady state oxygen evolution

The steady-state oxygen evolution was inhibited by the addition of $CdCl_2$ and incubation for 5 min in a biphasic way (Fig. 1A). A sharp 20% drop in the oxygen evolution occurred by the addition of <1 mM $CdCl_2$ (Fig. 1A, inset). Increased Cd^{2+} concentrations (>1 mM) resulted in further decrease of the oxygen evolution but with a less steep concentration dependence. At 10 mM $CdCl_2$, 55% of the oxygen evolution was inhibited (Fig. 1A). Seemingly, Cd^{2+} inhibits oxygen evolution in two concentration regimes, with one inhibition reaction occurring in the micromolar range (<1 mM) and the second inhibition reaction in the millimolar range (>1 mM). The inhibition was also investigated in salt-washed PSII membranes devoid of the 23- and 17-kDa subunits. In essence, the same inhibition pattern was found as in intact PSII membranes, but the inhibition was found to occur at much lower Cd^{2+} concentrations (Fig. 1A, inset). About 25% of the oxygen evolution was inhibited below 100 μM Cd^{2+}. The remaining oxygen evolution was also inhibited at lower concentrations than in the intact PSII membranes.

3.3. Cd^{2+} effects on flash-induced variable fluorescence

The rate of Q_A^- reoxidation was measured by following the decay of the variable fluorescence induced by a single flash. In untreated PSII, the flash-induced fluorescence decayed in three phases (Table 1, Fig. 2). The fast phase ($t_{½} \approx 1$ ms), reflects Q_A^- oxidation by Q_B/Q_B^-, when the Q_B site is filled with a quinone. The medium phase ($t_{½} \approx 20$ ms) reflects Q_A^- oxidation by Q_B, which first has to bind to the Q_B site; it thus represents Q_B binding and reports on the integrity of the Q_B site. The slow phase ($t_{½}$>1600 ms) reflects recombination between Q_A^- and the positively charged species in the OEC in PSII centers, which are not able to perform the forward electron transfer. A minor part of the flash-induced fluorescence did not decay during the 60-s measuring time (~10% of F_v is included in the slow phase in Table 1). The decay phases and their relative amplitudes are similar to what is commonly found in PSII enriched membrane preparations [38,43,44].

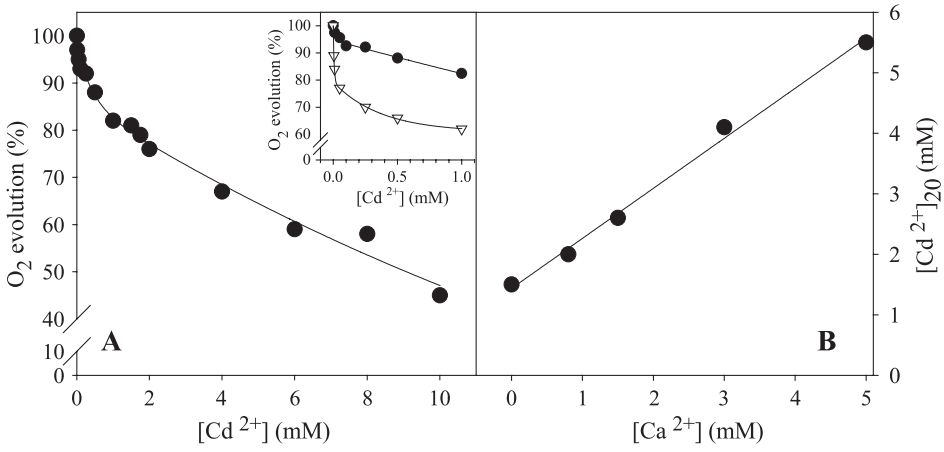

Fig. 1. (A) Inhibition of the steady-state oxygen evolution in intact PSII enriched membranes by the addition of $CdCl_2$. The inset is a magnification of the Cd^{2+}-induced inhibition occurring in the micromolar range in intact (black circles) or NaCl washed PSII membranes without the 23- and 17-kDa subunits (open triangles). (B) Oxygen evolution in the presence of both Cd^{2+} and Ca^{2+}. The curve shows how much $CdCl_2$ was needed to reach 20% inhibition of oxygen evolution, $[Cd^{2+}]_{20}$, in the presence of varying $CaCl_2$. Each measured point in A and B represents three independent O_2 evolution measurements. The error was ≤±5%.

Table 1
Flash-induced variable fluorescence decay halftimes and amplitudes for PSII particles incubated with different Cd^{2+} concentrations in the absence or presence of 20 μM DCMU or 5 mM Ca^{2+}. The amplitudes of the decay phases are presented as percent of the total amplitude of F_v in each particular measurement

No addition							
$[Cd^{2+}]$ (mM)	F_v/F_0[a]	Phase 1		Phase 2		Phase 3	
		$t_{½\ 1}$ (ms)±0.1	A (%)±5	$t_{½\ 2}$ (ms)±2	A (%)±3	$t_{½\ 3}$ (ms)	A (%)±2
0	100	1.1	61	22	20	>1600	19
1	78	1.4	57	26	21	>1600	22
5	63	1.9	44	38	22	>1600	34
10	55	3.3	31	50	25	>1600	44
DCMU							
$[Cd^{2+}]$ (mM)	F_v/F_0[a]	Phase 1		Phase 2		Phase 3	
		$t_{½\ 1}$ (ms) ±40	A (%) ±3	$t_{½\ 2}$ (s) ±0.1	A (%) ±3	$t_{½\ 3}$ (s)	A (%) ±3
0	100	280	25	2.1	63	>10	12
1	77	310	26	2.4	61	>10	13
5	71	300	25	2.4	53	>10	23
10	65	280	24	2.4	54	>10	24
Ca^{2+}							
$[Cd^{2+}]$ (mM)	F_v/F_0[a]	Phase 1		Phase 2		Phase 3	
		$t_{½\ 1}$ (ms)±0.1	A (%)±5	$t_{½\ 2}$ (ms)±4	A (%)±3	$t_{½\ 3}$ (ms)	A (%)±2
0	100	1.1	62	17	23	>1500	15
1	84	1.1	55	17	25	>1500	20
5	63	1.4	48	36	26	>1500	26

[a] The experiments in the absence and presence of DCMU were performed on different instruments (see Material and methods). To facilitate the comparison in the table, the total F_v/F_0 in the absence of Cd^{2+} was normalized to the same value.

By the addition of 0.1–10 mM $CdCl_2$, we observed several changes. These involved a lowering of the amplitude of the flash-induced fluorescence, F_v, slowdown of the decay phases and modification of their relative amplitudes (Table 1, Figs. 2 and 3). At 10 mM Cd^{2+}, the relative proportions between the three decay phases changed (Table 1). There was a large decrease of the amplitude of the fast phase (Q_A^- to Q_B/Q_B^-) and a large increase of the slow phase (Q_A^- recombination with the OEC, Table 1). The decay halftimes ($t_{½}$) of the two phases concerning Q_B and the Q_B binding site were significantly slowed down with the addition of Cd^{2+} from 1.1 and 22 ms (0 mM Cd^{2+}) to 3.3 and 50 ms (10 mM Cd^{2+}), respectively (Fig. 3 and Table 1). The kinetics of the slow phase, most likely reflecting recombination with the S_2 state in OEC, was not significantly altered. Taken together, these kinetic changes show that forward electron transfer from Q_A^- is severely hindered as a consequence of Cd^{2+}

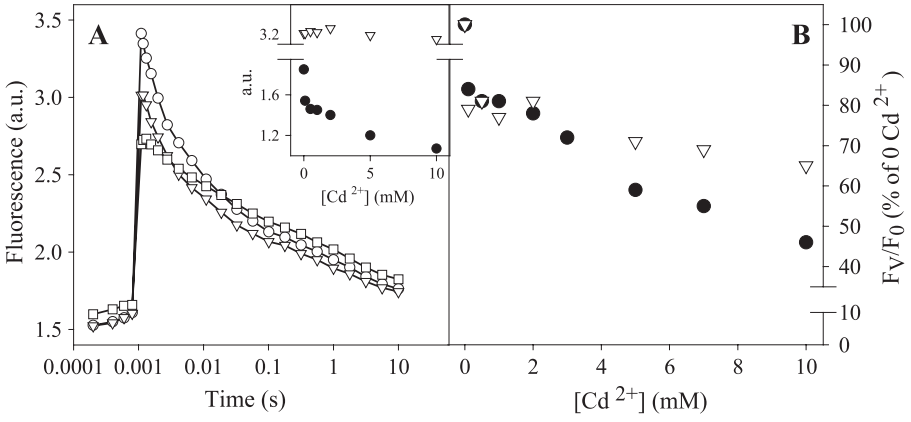

Fig. 2. (A) Flash-induced variable fluorescence decay measurements in the presence of 0 (circles), 1 (triangles) and 10 mM (squares) Cd^{2+}. The inset shows how the variable fluorescence amplitude, F_v, decreased with increasing Cd^{2+} concentration (black circles). It also shows that the maximal fluorescence F_{max} measured in the presence of dithionite remained constantly high at any Cd^{2+} concentration (open triangles). (B) The variable fluorescence presented as F_v/F_0 in absence (black circles) and presence of 20 μM DCMU (open triangles). The difference reflects the protective effect of DCMU in the millimolar Cd^{2+} concentration range.

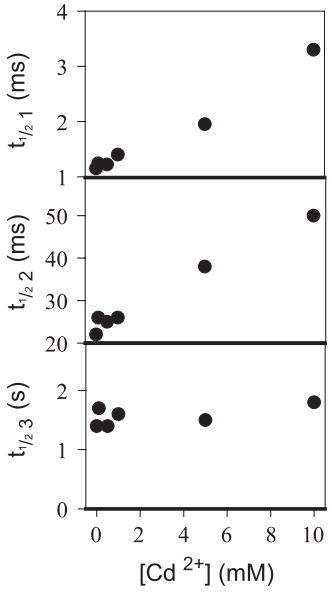

Fig. 3. Cd^{2+} dependence of the decay halftimes ($t_{½}$) of the flash-induced fluorescence. The fast and the medium decay phases (phase 1 and 2) were significantly slowed down, while the slow phase (phase 3) was not affected by the presence of $CdCl_2$. The decay halftimes were derived from 10–12 independent measurements. The accuracy for the determined halftimes is presented in Table 1.

incubation. Instead, a major fraction of photo-reduced Q_A is oxidized by recombination.

By the addition of Cd^{2+}, the amplitude of F_v decreased gradually (Table 1; Fig. 2A, inset). Similarly to the inhibition of steady state oxygen evolution, this decrease also occurred in a biphasic manner. In the presence of 1 and 10 mM Cd^{2+}, F_v decreased by 22% and 45%, respectively. There are several possible reasons for a loss of the F_v induced by a single flash. It could reflect that, in the inhibited fraction of PSII centers, (i) Q_A was rendered totally nonfunctional, (ii) less Q_A^- was formed on the flash (i.e., that the primary charge separation or electron transfer from pheophytin to Q_A was inhibited) or (iii) reoxidation of Q_A^- occurred faster than our fluorimeter could record (within <100 μs which was our first measuring point). From reduction experiments carried out with dithionite, the first option could be ruled out. The F_{max} level, measured after reduction of all functional Q_A in PSII by 17 mM dithionite, remained constant in samples with 0–10 mM Cd^{2+} (Fig. 2A, inset). It was also possible to rule out the second alternative from an EPR experiment (see below) where photo-accumulation at low temperature revealed that the amplitude of the $Q_A^-Fe^{2+}$ EPR signal remained constant even in the presence of 100 mM Cd^{2+}.

Instead, the lowered amplitude of the flash-induced F_v with increasing Cd^{2+} concentration probably reflects that part of Q_A^- was oxidized prior to our recording. This could be caused by faster forward electron transfer or by fast recombination to P_{680}^+ remaining on the donor side of PSII after the flash. The first alternative could be ruled out since all the fluorescence decay phases reflecting forward electron transfer actually were slowed down by the addition of cadmium (Table 1, Fig. 3). We therefore conclude that the amplitude of the flash-induced variable fluorescence was lost in the presence of Cd^{2+} due to the fast recombination of Q_A^- with an abnormally behaving component at the donor side of PSII. Thus, it is likely that the flash-induced fluorescence measurements revealed two sites of Cd^{2+} inhibition, one on the acceptor side slowing down and altering the forward electron transfer reactions and one on the donor side preventing the normal electron transfer reactions there.

By measuring the flash-induced fluorescence decay kinetics in the presence of DCMU, it is often possible to examine the donor side in PSII. DCMU binds to the Q_B site and blocks forward electron transfer from Q_A. Instead, Q_A^- is forced to recombine with the positively charge donor side components (after single flash, the dominating component is the S_2 state in the OEC) and the recombination kinetics reports on the integrity of the electron transfer chain on the donor side of PS II [38,44–47]. In the absence of Cd^{2+}, the flash-induced fluorescence in the presence of DCMU displayed a multi-exponential decay (Table 1) with two decaying phases ($t_{½} \approx 280$ ms and 2.1 s) and one non-decaying phase ($t_{½} > 10$ s). The 280-ms phase involved 25% of the fluorescence amplitude. A decay phase with this kinetics is frequently observed in this type of PSII preparations [38,44] and has been proposed to reflect recombination of Q_A^- with partially active Mn centers [38]. The dominating phase, with $t_{½} \approx 2.1$ s (63%), reflects recombination with the S_2 state of the Ca/Mn cluster. The very slow phase (12%), not decaying in the measuring time window of 10 s, probably corresponded to PSII centers that were in the S_0 state before the flash was applied [40,44].

The relative proportions and the decay halftimes (280 ms, 2.1 s, >10 s) of the kinetic phases were not significantly affected by the addition of 0.1–10 mM Cd^{2+} (Table 1). Moreover, similarly to the situation in the absence of DCMU, the total flash-induced F_v decreased with 23% in the 1 mM Cd^{2+} sample (Fig. 2B). However, in the sample incubated with 10 mM Cd^{2+}, F_v decreased to a smaller extent in the presence of DCMU than in its absence (Fig. 2B). Thus, DCMU seems to prevent the F_v amplitude decrease occurring in the millimolar Cd^{2+} concentration range.

3.4. Competition between Cd^{2+} and Ca^{2+}

Ca^{2+} and Cd^{2+} are known to compete in oxygen evolution assays [13,20,22]. Our fluorescence analysis indicated that there are several modes for Cd^{2+} inhibition of PSII electron transfer. Therefore, we investigated if Ca^{2+} could replace the bound Cd^{2+} ion(s) in both assay systems. The steady-state oxygen evolution was measured in the presence of both ions. The PSII samples were treated with 0–10 mM $CdCl_2$ in the presence of 0.8–5.0 mM $CaCl_2$. In the presence of Ca^{2+}, the biphasic cadmium inhibition curve (Fig. 1A) changed into a more simple inhibition pattern with increasing concentra-

tions of calcium (not shown). When more than 1.5 mM Ca^{2+} was added, the high affinity Cd^{2+} inhibition that occurred at [Cd^{2+}]<1 mM disappeared. Above 3 mM Ca^{2+}, the low affinity inhibition occurring at [Cd^{2+}]>1 mM was also accessed. Direct interpretation of these measurements was, however, complex, since Ca^{2+} also activates the oxygen evolution with ca 10% in the control material. Therefore, we have refrained from a more rigorous kinetic analysis of our competition data. Such studies are better done after complete equilibrium in the Ca^{2+} site has been reached, as discussed in Ref. [22]. Despite this, our experiment shows that, when the Ca^{2+} concentration was increased, it was necessary to increase the Cd^{2+} concentration significantly to reach 20% inhibition (Fig. 1B). Thus, it is clear that Ca^{2+} affected the Cd^{2+} inhibition. The effect seems to be a competitive inhibition in the micromolar inhibition range. This is similar to what has been found earlier for the site close to the OEC [22] and we conclude that our high-affinity Cd^{2+} site (<1 mM Cd^{2+}) probably reflects this site. The effect of Ca^{2+} on Cd^{2+} inhibition at higher Cd^{2+} concentrations is less pronounced and probably of different nature.

3.5. Reversibility of Cd^{2+} inhibition

To test if the Cd^{2+} inhibition was reversible, a procedure was developed to wash away excess and bound Cd^{2+}. The effect of incubation with 2 mM Cd^{2+} concentration was studied. We also performed a combined washing and competition experiment by adding 5 mM $CaCl_2$ to the assay after the washing procedure. The results are compiled in Fig. 4. The washing itself resulted in a small decrease of oxygen evolution (9%). In the sample incubated with 2 mM Cd^{2+}, the washing did not increase the oxygen evolution back to the control level. However, when Ca^{2+} was added after the wash, the activity was recovered almost completely. We see two explanations for this. First, it might be very difficult to remove Cd^{2+} from the site occupied at 2 mM Cd^{2+} simply by washing and Ca^{2+} is needed to outcompeted Cd^{2+} from this site. Second, Cd^{2+} might displace Ca^{2+} from the site and activity can only be regained if Ca^{2+} is present in the assay medium.

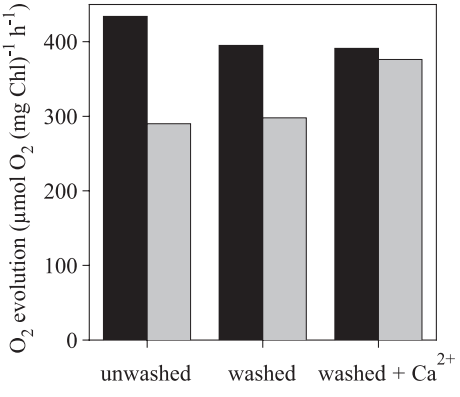

Fig. 4. Reversibility of the Cd^{2+} treatment of PSII particles. PSII enriched membranes, incubated with 0 (black) or 2 mM Cd^{2+} (grey), were washed to remove bound and excess Cd^{2+} (see Materials and methods). The oxygen evolution was then compared between the unwashed (left) and the washed (middle) PS II samples. The washed samples were measured with and without the addition of 5 mM $CaCl_2$ (right).

To conclude, our washing experiments indicate that Cd^{2+} and Ca^{2+} efficiently compete in the high-affinity site (accessed by 2 mM Cd^{2+}). Cd^{2+} can only be removed from this site and activity be regained in the presence of a competing agent, in our case Ca^{2+}. Performing experiments with higher concentrations of Cd^{2+}, also interacting with the low affinity site, were complicated by the fact that incubation with higher salt concentration and washing probably removed the 17-kDa extrinsic subunit (see below). Therefore, this type of experiment was excluded from our analysis.

3.6. EPR studies of Cd^{2+} effects on individual redox components in PSII

Measurements of oxygen evolution and variable fluorescence provide information about the number of Cd^{2+} binding sites and the approximate binding constants. However, these assays are less informative concerning the exact site for the binding and the mechanism of the inhibition. To probe these in further detail, we turned to EPR spectroscopy, which can provide details about the behavior of almost every redox component in the PSII reaction center. Such analysis has earlier proven very useful in studies of Cu^{2+}-induced inhibition of PSII [29] and is here applied for the first time on Cd^{2+}-induced inhibition.

3.6.1. Effect of Cd^{2+} on the $Q_A^-Fe^{2+}$ EPR signal

The fluorescence analysis revealed a Cd^{2+} inhibition site that affected the electron transfer from Q_A^-. Therefore, we investigated how Cd^{2+} affected the amplitude of the light-induced EPR signal from Q_A^-. This signal is known as the $Q_A^-Fe^{2+}$ signal and reflects a magnetic interaction between the reduced Q_A and the nearby acceptor side Fe^{2+} ion [42,48,49]. Thus, the observation of the EPR signal demands the presence of both these components. The signal is very small and at g=1.9, which makes it difficult to detect due to severe spectral overlap with the large radical signal from $Y_D^{\cdot}$ [42,48,49]. This can be overcome by the addition of formate that is known to modify the $Q_A^-Fe^{2+}$ signal to an easier detectable form at g=1.82 (together with a trough at $g \approx 1.7$), which also has a much larger amplitude than the signal in samples without formate [48,49]. Therefore, we have added formate to the Cd^{2+}-treated samples.

The shape and size of the $Q_A^-Fe^{2+}$ signal are not changed, even by incubation with 100 mM $CdCl_2$ (Fig. 5A and C). In this experiment, Q_A was reduced by illumination of the sample at 200 K. Consequently, we can conclude that the light-induced electron transfer between P_{680} and Q_A is not blocked and that Cd^{2+} binding in PSII apparently is localized apart from P_{680}, pheophytin or Q_A.

Although Cd^{2+} does not inhibit the reduction of Q_A, incubation with 100 mM Cd^{2+} modifies the EPR appearance

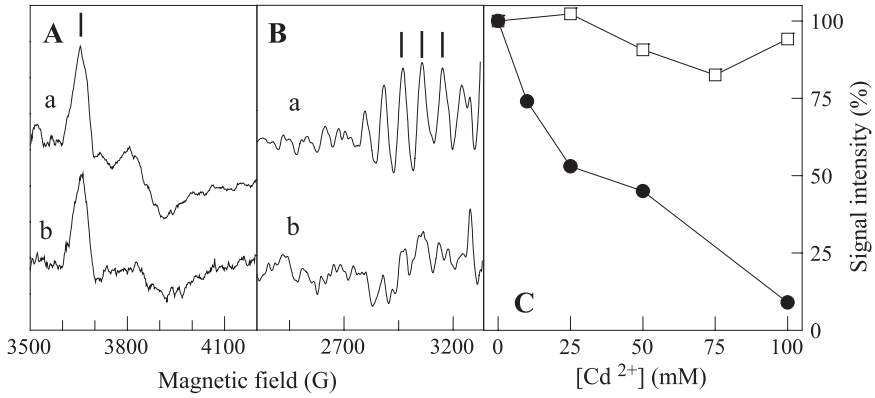

Fig. 5. Effect of Cd^{2+} on the formation of different EPR signals. Spectra a and b in panel A and B represent the formation of the EPR signal in the absence or presence of 100 mM $CdCl_2$, respectively. (A) Induction of the $Q_A^-Fe^{2+}$ signal. (B) Formation of the S_2 state ML signal. The bars in A and B indicate the peaks used to determine the spectral intensity of the $Q_A^-Fe^{2+}$ signal and S_2 state ML signal, respectively. (C) Cd^{2+} concentration dependence of the formation of the $Q_A^-Fe^{2+}$ (open squares) and the S_2 state ML signal (closed circles). All spectra were recorded in the presence of 50 mM Na-formate to enhance the amplitude of the $Q_A^-Fe^{2+}$ signal. $CdCl_2$ was added 5 min before the freezing. The EPR signals were induced by continuous illumination at 200 K. All spectra represent illuminated minus dark difference spectra. EPR settings: microwave frequency 9.41 GHz, modulation amplitude 15 G. (A) Microwave power 32 mW; temperature 4 K; (B) microwave power 16 mW; temperature 7 K.

of Q_A^- in two significant ways. First, Cd^{2+} shifts the spectral form of the $Q_A^-Fe^{2+}$ signal to the g=1.82 form, even in the absence of formate (Fig. 6). Such modifications have been observed before and have been found to be induced by herbicides that bind in the Q_B site or by formate that binds to the Fe^{2+} [48,49]. Consequently, this change in Cd^{2+}-incubated samples probably reflects Cd^{2+} binding close to one or both of Q_B and Fe^{2+} on the acceptor side. Interestingly, after incubation with 100 mM $CdCl_2$, illumination at 200 K induced a fraction (6%) of Q_A^- that was magnetically uncoupled from the non-heme iron (not shown). The free radical of Q_A^- gives rise to a non-perturbed radical EPR signal that is easily recognized by its

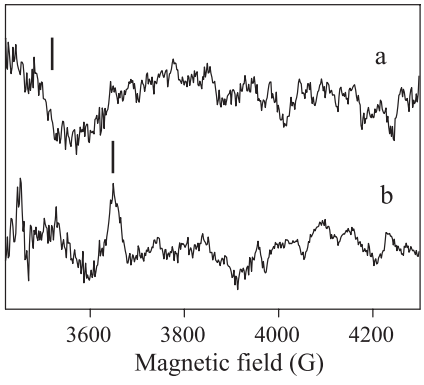

Fig. 6. Alteration of the spectral shape of the $Q_A^-Fe^{2+}$ EPR signal by the addition of Cd^{2+}. It should be noted that these spectra are recorded in the absence of formate, which explains the low signal to noise ratio [48]. In the control sample (top spectrum), the illumination results in the formation of the S_2 state ML signal (part of this is visible in the spectrum as the peaks around 4000 G) while the expected EPR signal from $Q_A^-Fe^{2+}$ is at g=1.9 (bar in the top spectrum) which is located at the shoulder from $Y_D^{\cdot}$. Consequently the small signal from $Q_A^-Fe^{2+}$ is not observable. In the presence of 100 mM Cd^{2+} the $Q_A^-Fe^{2+}$ signal is shifted to g=1.82 (bar in the bottom spectrum) and the spectrum is clearly observed. EPR conditions as in Fig. 5A.

g-value (g=2.0044) and spectral width (9.5–10.0 G) [50,51]. It reflects that the heavy metal binding is close enough on the acceptor side to break the magnetic interaction between Q_A^- and Fe^{2+}. The formation of this signal was observed also as a consequence of Cu^{2+} binding to PSII [29].

3.6.2. Effect of Cd^{2+} on the S_2 state ML signal

Fig. 5B shows the formation, by illumination at 200 K, of the S_2 state ML EPR signal from the OEC. The formation of this signal was almost completely abolished by addition of 100 mM Cd^{2+}. The Cd^{2+}-concentration dependence of the S_2 state ML signal formation is presented in Fig. 5C. This shows that Cd^{2+} inhibited the formation of the S_2 state although the primary charge separation and reduction of Q_A still remained fully functional over the same concentration of Cd^{2+}.

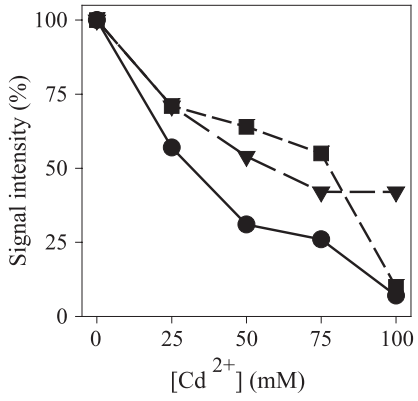

Fig. 7. Dependence of the amplitude of the S_2 state ML EPR signal on the concentration of Cd^{2+} in the absence (circles) or presence of 100 μM DCMU (triangles) or 25 mM Ca^{2+} (squares). Signal intensity calculated as described in Fig. 5.

3.6.3. Effects of DCMU and Ca^{2+} on the Cd^{2+}-induced changes in the S_2 state ML signal

We also tested how DCMU or Ca^{2+} influenced the formation of the S_2 state ML signal at various Cd^{2+} concentrations. The results are shown in Fig. 7. In the presence of 25 mM Ca^{2+}, 30% and 50% of the lost ML signal are regained in the presence of 25 and 50 mM Cd^{2+}, respectively. This is in agreement with all other measurements and shows that Ca^{2+} and Cd^{2+} compete for the same site in the OEC. It also confirms that Ca^{2+} does not outcompete Cd^{2+} in all inhibitory sites. The results in Fig. 7 suggest that Ca^{2+} does not compete at all at 100 mM Cd^{2+}. However, at these high ionic strengths the 23- and 17-kDa extrinsic subunits from the OEC are probably lost. Our oxygen evolution measurements revealed that Cd^{2+} binds much more efficiently in the absence of these subunits (Fig. 1A, inset). It is thus likely that Ca^{2+} competes less efficiently at higher Cd^{2+} concentrations due to secondary effects caused by the high ionic strength. Probably this effect is gradual over the Cd^{2+} concentration range and at 100 mM Cd^{2+} the chosen Ca^{2+} concentration (25 mM) is too low to allow successful competition.

Interestingly, DCMU had similar effects as Ca^{2+} (Fig. 7) and in the presence of 100 μM DCMU, the S_2 state ML signal was induced to a much higher extent than in the absence of DCMU. Even in the presence of 100 mM Cd^{2+}, 42% of the ML signal could be induced by illumination at 200 K. DCMU binds in the Q_B binding site and is normally not considered to bind on the donor side of PSII. Thus, the observation that DCMU hinders Cd^{2+} to exert its function on the S_2 state ML signal is interesting but difficult to explain, and different alternatives will be discussed in Discussion.

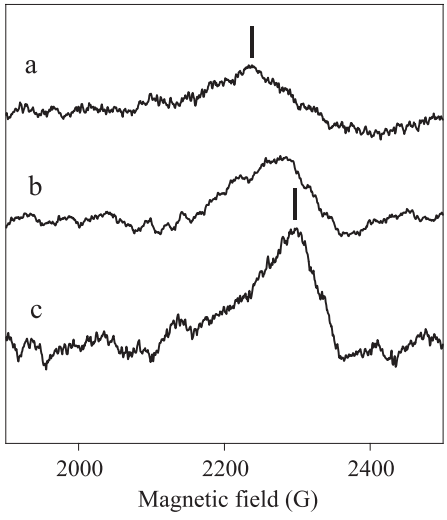

Fig. 8. Effect of Cd^{2+} on the oxidation state of Cyt b_{559}. Spectra were detected in the presence of (a) 0, (b) 50 and (c) 100 mM $CdCl_2$. The spectra show the g_z region (g values 2.96 and 2.93 are indicated by bars) of the Cyt b_{559} signal recorded after incubation with $CdCl_2$. EPR settings: microwave frequency 9.41 GHz; microwave power 5 mW; temperature 15 K; modulation amplitude 15 G.

3.6.4. Effects of Cd^{2+} on Cyt b_{559}

Cyt b_{559} is sensitive to many structural and functional changes in PSII. This also holds for the presence of Cd^{2+}. Fig. 8 shows how the EPR spectrum of Cyt b_{559} changes upon the addition of Cd^{2+}. In the absence of Cd^{2+}, the EPR spectrum in the g_z region of Cyt b_{559} is small and dominated by the oxidized low-potential form of the cytochrome. The spectrum is normal for PSII membrane preparations and represents ca 25–30% of the available Cyt b_{559} being in the oxidized low potential form [42,52]. The remaining cytochrome is reduced and it is in the high and intermediate potential form.

When Cd^{2+} is added, the EPR spectrum from the oxidized low-potential form grows bigger with increasing concentrations of Cd^{2+}. In the presence of 100 mM Cd^{2+} the spectrum is more than two times larger than in the control sample and shows that Cd^{2+} effects the formation of low-potential Cyt b_{559} from the high-potential form in a large fraction of the centers. This change occurs in a Cd^{2+}-concentration-dependent manner.

4. Discussion

This study shows that Cd^{2+} has a complex pattern of interactions with PSII. There are several Cd^{2+}-induced inhibitions or modifications of PSII function. Cd^{2+} alters the redox potential form of Cyt b_{559}; it inhibits electron transfer from Q_A^- to Q_B; it modifies the spectral properties of Q_A^-; and it inhibits formation of the S_2 state in the oxygen evolving cycle and consequently the oxygen evolution in PSII. We will discuss our results concerning these sites independently.

4.1. Interaction of Cd^{2+} with Cyt b_{559}

Cyt b_{559} is present in the core of PSII [3–5] and can take several different redox potentials [53,54]. In PSII enriched membranes, the high potential form dominates but in 25–30% [52,53] of the centers Cyt b_{559} is in the low-potential form (this was the case in our preparation (Fig. 8). When PSII was incubated with increasing concentrations of Cd^{2+}, this resulted in a gradual change to the low-potential form as revealed by the increased oxidation level of the Cyt b_{559}. The g_z value of the low potential form is shifted from 2.96 (which is normal for untreated PSII) to 2.93 (Fig. 8), which is similar to the g_z value of purified low potential Cyt b_{559} [52]. A change from the high potential form to the low-potential form is frequently observed in PSII [52,53]. It often reflects removal of the Ca/Mn cluster or the extrinsic subunits shielding the OEC and/or binding of reactive agents in the vicinity of Cyt b_{559}. Cd^{2+} binds at several places in PSII and it can be difficult to ascertain which site is involved in the shift of the potential of Cyt b_{559}. However, we propose that the redox potential shift reflects removal of the 17-kDa subunit from the donor side of PSII. Removal of this subunit,

correlated to a shift of the redox potential of Cyt b_{559}, was found to occur when PSII was incubated with 10 mM Cu^{2+} [29]. It is likely that incubation with even higher amounts of $CdCl_2$ also resulted in loss of this subunit. It has also been proposed that release of Ca^{2+} can transform the high-potential form to the low-potential form of Cyt b_{559} [55]. Our short Cd^{2+} treatment probably involves displacement of Ca^{2+} in a fraction of the centers (see below). Therefore, we conclude that the shift of Cyt b_{559} to the low-potential form probably reflects both the disturbance of the protein structure on the donor side of PSII and the binding of Cd^{2+} in the Ca^{2+} site involved in oxygen evolution.

4.2. Interaction of Cd^{2+} with the acceptor side of PSII

Several results indicate that Cd^{2+} binds at the acceptor side of PSII and it is possible to draw conclusions about this site. The light-induced charge separation between P_{680} and Q_A, studied by low temperature illumination (measured as the amplitude of the $Q_A^-Fe^{2+}$ EPR signal; Fig. 5C), remained fully functional in the presence of very high concentrations of Cd^{2+}. This indicates that Cd^{2+} did not affect Q_A itself. Instead, the competitive effect of DCMU that leads to partial recovery of the S_2 state ML signal in the presence of Cd^{2+} suggests that the acceptor-side Cd^{2+} binds in or close to the Q_B binding site. This is corroborated by the fluorescence measurements that reveal that Cd^{2+} slows down the kinetics in forward electron transfer from Q_A^- either by perturbing the function of Q_B or by modifying the electron transfer at the level of the reduction of Q_B.

Structural changes induced by binding of Cd^{2+} at the acceptor side of PSII are also revealed by the change in the spectral shape of the $Q_A^-Fe^{2+}$ signal. This complex EPR signal, which demands structural integrity of both Q_A and the non-heme Fe^{2+} situated 7 Å away, is shifted to another form with a different g value (Fig. 6). In addition, a tiny fraction of Q_A^- became magnetically decoupled from the Fe^{2+}. The latter effect is similar, but smaller in magnitude, to the magnetic decoupling of Q_A^- and Fe^{2+} observed by incubation with Cu^{2+} [29]. In that case, it was speculated that Cu^{2+} actually displaced the Fe^{2+} by ligation to the histidine residues that coordinate the Fe^{2+} ion [29].

It is possible that Cd^{2+} could bind in a similar way, displacing Fe^{2+}. However, the small fraction of magnetically uncoupled Q_A^-, and the clear effect of Cd^{2+} on the $Q_A^-Fe^{2+}$ signal (Fig. 6), suggests that this is not the primary reaction. Instead, we put forward an alternative proposal. The idea stems from detailed studies of the Cd^{2+} inhibition of the electron transfer between Q_A^- and Q_B in purified reaction centers from the purple bacterium *Rb. sphaeroides* [17,19,21,24]. It was found that Cd^{2+} binds to two histidine residues in the H subunit [24]. These histidines constitute the entry point for protons participating in the protonation of reduced Q_B. Cd^{2+} binding blocks this entry point and thereby the electron transfer is slowed down. The two histidine residues do not have known, directly homologous partners in PSII. Despite this, a similar phenomenon might prevail since Q_B is reduced in a quite similar fashion in PSII. Thus, Cd^{2+} could bind to a site involved in protonation of Q_B. The site would be located in one of the core subunits of PSII, thereby identification becomes possible by approaches involving Cd^{2+} induced inhibition. In this respect, it is interesting that D1-His252 was pointed out to be in hydrogen bonding contact to D1-Ser264, which is directly connected to Q_B [5]. This led to the suggestion [5] that D1-His252 might be a candidate for residues involved in the protonation pathway of Q_B. If this holds true, D1-His252 could be involved in the low-affinity binding of Cd^{2+} thereby affecting electron transfer between the quinone acceptors and the magnetic interactions between Q_A^- and the Fe^{2+}, which are all in the immediate vicinity.

4.3. Cd^{2+} binding to the donor side

In many studies of Cd^{2+} inhibition, the inhibition of steady state oxygen evolution has been measured. This provides information about the entire electron transport chain between OEC and Q_B and allows determination of binding constants of Cd^{2+}, but is less informative concerning the exact site and the mechanism of the inhibition. We have turned to single flash-induced variable fluorescence and EPR measurements to obtain a more detailed picture.

By the application of illumination at 200 K on PSII, only one charge separation can take place because the Q_A^- to Q_B electron transfer is blocked at this temperature [41]. EPR analysis revealed that the yield of Q_A photo-reduction was independent from the applied Cd^{2+} concentration. Thus, the primary charge separation is operational and it is safe to conclude that Cd^{2+} does not interfere with P_{680} or the intermediary pheophytin acceptor.

In contrast, our flash-induced fluorescence studies showed that a large fraction of the amplitude of F_v was lost when Cd^{2+} was present. This occurred in two concentration regimes; part of the F_v was lost due to Cd^{2+} interaction in a site with high affinity while a larger part of F_v was lost due to interaction in a site with low affinity. The yield of the fluorescence in the presence of dithionite and the light-induced $Q_A^-Fe^{2+}$ EPR signal were both unchanged in presence of Cd^{2+}. Thereby, we can exclude that Q_A was lost or that Q_A reduction was inhibited, leading to lower flash-induced F_v. Instead, we conclude that recombination occurs in the single flash measurement before we actually can detect the fluorescence.

Our measuring system allows detection of the fluorescence only 100 μs after the flash. If recombination was the reason for the lost fluorescence, it must have occurred within these 100 μs. Recombination reactions from Q_A^- often involve the S-states in OEC or $Y_Z^{\cdot}$ (in case the Ca/Mn cluster is inactive) and all these reactions are much slower than 100 μs. We therefore conclude that, in the presence of Cd^{2+}, a large fraction of flash-induced Q_A^- recombines with the oxidized primary donor P_{680}^+ remaining during as much

as 100 μs. This is unusual and suggests that no electron can arrive from Y_Z fast enough to prevent recombination. Thus, the flash-induced fluorescence measurement indicates that Cd^{2+} actually inhibits the electron transfer from Y_Z to P_{680}^+ and that Cd^{2+} affects this in both the high-affinity and the low-affinity site. Again, this is similar as Cu^{2+}, which was found to inhibit electron transfer from Y_Z [29], preventing Y_Z oxidation.

Inhibition of Y_Z to P_{680}^+ electron transfer can also explain the inhibition of oxygen evolution at higher Cd^{2+} concentrations (>1.5 mM, i.e., the low-affinity site for Cd^{2+}) and the inhibition of the S_2 state ML EPR signal formation. However, in the case of the high-affinity Cd^{2+} site of the oxygen evolution inhibition and the large fraction of the Cd^{2+}-induced inhibition of the S_2 state ML signal, Ca^{2+} was able to compete successfully with Cd^{2+}. This is different from the loss of the flash-induced F_v, where the competition between Ca^{2+} and Cd^{2+} did not increase the amplitude (Table 1), indicating that Ca^{2+} competes badly or not at all with Cd^{2+} in this site. We must consequently conclude that Cd^{2+} has at least two effects on the donor side of PSII; it blocks oxidation of Y_Z in a Ca^{2+}-independent manner and it blocks the OEC in a Ca^{2+}-dependent manner.

It is interesting to discuss the two sites that seem to affect donor-side reactions. In one of the sites, Ca^{2+} competes with Cd^{2+}. Binding of Cd^{2+} in this site results in inhibition of the oxygen evolution in about 20% of the PSII centers and occurs with high affinity. Competition with Ca^{2+} is also successful to regain a fraction of the lost S_2 state ML amplitude. The competition between Ca^{2+} and Cd^{2+} and the high affinity involved in the inhibition of the oxygen evolution strongly suggest that the site involves exchange of Ca^{2+} and Cd^{2+} in the Ca/Mn cluster [5,22]. The reason for the incomplete exchange is the short time used (5 min) compared to the several hours it takes to reach equilibrium in this site [22]. With the present structural knowledge [5] that the Ca^{2+} ion is situated ca 6.5 Å away from the phenolic oxygen of Y_Z and is then the closest metal to Y_Z, the results are easy to understand. The volume between the Ca^{2+} and Y_Z seems to be devoid of protein. Instead, it probably contains water molecules and it is likely that one or several of these are involved in hydrogen bonding networks around the phenolic proton of Y_Z or other critical side chains in the neighborhood (albeit this cannot be ascertained at the present structural resolution). Binding of Cd^{2+} to this site is likely to perturb such fragile structures, thereby probably slowing down or even preventing Y_Z oxidation. In this context, it is also important that Y_Z oxidation is severely slowed down (or even totally hindered even if this latter statement has been questioned in several reports [56,57]) as a consequence of Ca^{2+} depletion [58]. It is not unlikely that the reason for this inhibition is that deprotonation of Y_Z is prevented due to perturbation of the immediate structure around the phenolic proton.

Cd^{2+} inhibition also occurred with low affinity and affected both oxygen evolution, F_v, the S_2 state ML signal and acceptor-side kinetics. Here Cd^{2+} could not be outcompeted by Ca^{2+} for any of the measured parameters although Cd^{2+} binds less well. Thus, these two sites are not the same as the high-affinity site and we propose that there are two low-affinity sites involved in Cd^{2+} binding to PSII. One has been discussed above and is proposed to occur at the acceptor side, maybe close to the proton chain between Q_B and the environment. Moreover, our results indicate that there is a low affinity site also at the donor side of PSII. Binding of Cd^{2+} to this site also results in decreased formation of the S_2 state ML signal and decreased flash-induced variable fluorescence, F_v, due to recombination.

It is not unlikely that this site reflects the Cd ion that was found in the X-ray structure in [3]. This Cd^{2+} site was discussed by Rutherford and Faller [9] and was proposed to maybe involve a H^+ channel (or H-bonding chain) from the site for water oxidation to the lumenal side of PSII. This is an interesting idea and modified proton release from the OEC due to Cd^{2+} binding could well modify the turnover of Y_Z and stall the turnover of the OEC. In this context, it is again worthwhile to point out that the recent X-ray structure [5] prompted the authors to propose some residues that might be involved in proton release from the OEC. Thus, it is not impossible that the low-affinity binding of Cd^{2+} we observe reflects Cd^{2+}-binding to proton channels on both the acceptor side and the donor side of PSII.

However, this is not necessarily the only explanation of our data. DCMU can partially prevent the Cd^{2+}-induced effects also on the donor side of PSII. This is surprising since DCMU binds in the Q_B site and not on the donor side of PSII. There are, however, many cases in PSII where binding of an agent on one side of the membrane affects components on the other side of the membrane. The most well-known effects involve modification of Cyt b_{559}, which changes to the low-potential form when extrinsic subunits are lost from PSII [52], when Ca^{2+} is removed from the OEC [55], etc. Thus, there are tight connections between donor-side- and acceptor-side-located components. These probably involve the membrane spanning helices and, for example, Y_Z and Q_B bind to the very same helix at different sides of the membrane [5,59]. Therefore, it is not unreasonable to propose that DCMU binding in the Q_B site, which prevents the binding of Cd^{2+} to its site at the acceptor side, affects the Cd^{2+}-induced modifications of donor-side electron transfer reactions. This would occur through helix-assisted transmembrane signaling. At present, we cannot judge which alternative is true, but further studies of the low-affinity binding of Cd^{2+} might help in probing one or more of the H^+ channels involved in PSII catalyzed reactions.

5. Conclusion

Our results indicate that Cd^{2+} has multiple effects on both the donor side and the acceptor side of PSII. On the

donor side, the presence of Cd^{2+} inhibits oxygen evolution in a high-affinity site by competition with Ca^{2+}. In our study, this inhibition only encompasses ca 20% of the PSII centers and earlier work has revealed that it takes several hours for Cd^{2+} to reach equilibrium in this site. Cd^{2+} also inhibits, in a similar way as Cu^{2+}, the oxidation of Y_Z in a site where Ca^{2+} seemingly does not compete. On the acceptor side of PSII, Cd^{2+} has several effects, all indicating that Cd^{2+} binds to, or close to, the Q_B binding site and not in the vicinity of Q_A. It is likely that the site is situated close to the acceptor-side Fe^{2+} and the binding might have properties similar to the Cd^{2+} known to inhibit the entry of a proton channel involved in protonation of reduced Q_B in purple bacteria.

Binding of metal ions to several sites in PSII is not a property exclusive to Cd^{2+}. Instead, this is the general picture when assays that are detailed enough have been used, and all of Ca^{2+}, Cu^{2+} Zn^{2+} [27] and Cd^{2+} have been shown to bind in sites on both the acceptor side and the donor side of PSII [27,29,56]. Some of these sites have similar properties and seem to be the same for all four ions.

Acknowledgments

The financial support from the Swedish Research Council, DESS, the Swedish Energy Agency and the EC Programme “Improving Research Potential and the Socio-economic Knowledge Base” (MCFI-2000-01465) (G.B.) is gratefully acknowledged. We are grateful to Dr. Peter Faller for stimulating discussions and providing complete documentation of recent work in his laboratory.

References

[1] B.A. Diner, G.T. Babcock, Structure, dynamics, and energy conversion efficiency in photosystem II, in: D.R. Ort, C.F. Yocum (Eds.), Oxygenic Photosynthesis: The Light Reactions, Kluwer Academic Publishers, Dordrecht, The Netherlands, 1996, pp. 213–247.

[2] J. Barber, Photosystem II: the engine of life, Q. Rev. Biophys. 36 (2003) 71–89.

[3] A. Zouni, H.T. Witt, J. Kern, P. Fromme, N. Krauss, W. Saenger, P. Ort, Crystal structure of photosystem II from *Synechococcus elongatus* at 3.8 angstrom resolution, Nature 409 (2001) 739–743.

[4] N. Kamiya, J.-R. Shen, Crystal structure of oxygen-evolving photosystem II from *Thermosynechococcus vulcanus* at 3.7-angstrom resolution, Proc. Natl. Acad. Sci. U. S. A. 100 (2003) 98–103.

[5] K.N. Ferreira, T.M. Iversson, K. Maghlaoui, J. Barber, S. Iwata, Architecture of the photosynthetic oxygen-evolving center, Science 303 (2004) 1831–1838.

[6] R.M. Cinco, J.H. Robblee, A. Rompel, C. Fernandez, V.K. Yachandra, K. Sauer, M.P. Klein, Strontium EXAFS reveals the proximity of calcium to the manganese cluster of oxygen-evolving photosystem II, J. Phys. Chem., B 102 (1998) 8248–8256.

[7] M.J. Latimer, V.J. DeRose, V.K. Yachandra, K. Sauer, M.P. Klein, Structural effects of calcium depletion on the manganese cluster of photosystem II: determination by X-ray absorption spectroscopy, J. Phys. Chem., B 102 (1998) 8257–8265.

[8] R.M. Cinco, K.L.M. Holman, J.H. Robblee, J. Yano, S.A. Pizarro, E. Belacchio, K. Sauer, V.K. Yachandra, Calcium EXAFS establishes the Mn–Ca cluster in the oxygen-evolving complex of photosystem II, Biochemistry 41 (2002) 12928–12933.

[9] A.W. Rutherford, P. Faller, The heart of photosynthesis in glorious 3D. Trends Biol. Sci. 26 (2001) 341–344.

[10] M.B. Bazzaz, Govindjee, Effects of cadmium nitrate on spectral characteristics and light reactions of chloroplasts, Environ. Lett. 6 (1) (1974) 1–12.

[11] M.A. Van Duijvendijk-Matteoli, G.M. Desmet, Inhibitory action of cadmium on donor side of photosystem II in isolated-chloroplasts, Biochim. Biophys. Acta 408 (1975) 164–169.

[12] T.-A. Ono, Y. Inoue, Roles of Ca^{2+} in O_2 evolution in higher-plants photosystem II—effects of replacement of Ca^{2+} site by other cations, Arch. Biochem. Biophys. 275 (1989) 440–448.

[13] C.M. Waggoner, C.F. Yocum, Calcium activated oxygen evolution, in: M. Baltscheffsky (Ed.), Curr. Res. Photosynth., vol. I, Kluwer Academic Publishers, Dordrecht, The Netherlands, 1990, pp. 733–736.

[14] J. Matysik, H.J. van Gorkom, H.J.M. de Groot, Substitution of calcium by cadmium in photosystem II complex, in: G. Garab (Ed.), Photosynthesis: Mechanisms and Effects, vol. II, Kluwer Academic Publishers, Dordrecht, The Netherlands, 1998, pp. 1423–1426.

[15] B. Geiken, J. Masojidek, M. Rizzuto, M.L. Pompili, M.T. Giardi, Incorporation of [S-35]methionine in higher plants reveals that stimulation of the D1 reaction centre II protein turnover accompanies tolerance to heavy metal stress, Plant Cell Environ. 21 (1998) 1265–1273.

[16] E. Franco, S. Alessandrelli, J. Masojidek, A. Margonelli, M.T. Giardi, Modulation of D1 protein turnover under cadmium and heat stresses monitored by [S-35]methionine incorporation, Plant Sci. 144 (1999) 53–61.

[17] M.L. Paddock, M.S. Graige, G. Feher, M.Y. Okamura, Identification of the proton pathway in bacterial reaction centers: inhibition of proton transfer by binding of Zn^{2+} or Cd^{2+}, Proc. Natl. Acad. Sci. U. S. A. 96 (1999) 6183–6188.

[18] B. Szalontai, L.I. Horvath, M. Debreczeny, M. Droppa, G. Horvath, Molecular rearrangements of thylakoids after heavy metal poisoning, as seen by Fourier transform infrared (FTIR) and electron spin resonance (ESR) spectroscopy, Photosynth. Res. 61 (1999) 241–252.

[19] H.L. Axelrod, E.C. Abresch, M.L. Paddock, M.Y. Okamura, G. Feher, Determination of the binding sites of the proton transfer inhibitors Cd^{2+} and Zn^{2+} in bacterial reaction centers, Proc. Natl. Acad. Sci. U. S. A. 97 (2000) 1542–1547.

[20] J. Matysik, A. Alia, G. Nachtegaal, H.J. van Gorkom, A.J. Hoff, H.J.M. de Groot, Exploring the calcium-binding site in photosystem II membranes by solid-state Cd-113 NMR, Biochemistry 39 (2000) 6751–6755.

[21] S. Keller, J.T. Beatty, M. Paddock, J. Breton, W. Leibl, Effect of metal binding on electrogenic proton transfer associated with reduction of the secondary electron acceptor (Q(B)) in *Rhodobacter sphaeroides* chromatophores, Biochemistry 40 (2001) 429–439.

[22] J.S. Vrettos, D.A. Stone, G.W. Brudvig, Quantifying the ion selectivity of the Ca^{2+} site in photosystem II: evidence for direct involvement of Ca^{2+} in O_2 formation, Biochemistry 40 (2001) 7937–7945.

[23] J. Voigt, K. Nagel, Metabolic alterations associated with Cd-tolerance in *Chalmydomonas* cells, Biol. Chem. Hoppe-Seyler 372 (1991) 719–720.

[24] M.L. Paddock, L. Sagle, A. Tehrani, J.T. Beatty, G. Feher, M.Y. Okamura, Mechanism of proton transfer inhibition by Cd^{2+} binding to bacterial reaction centers: determination of the pK(A) of functionally important histidine residues, Biochemistry 42 (2003) 9626–9632.

[25] N. Mohanty, I. Vass, S. Demeter, Copper toxicity affects photosystem II electron-transport at the secondary quinone acceptor, Q_B, Plant Physiol. 90 (1989) 175–179.

[26] N. Mohanty, I. Vass, S. Demeter, Impairment of photosystem 2 activity at the level of secondary quinone electron-acceptor in chloroplasts treated with cobolt, nickel and zinc ions, Physiol. Plant. 76 (1989) 386–390.
[27] A. Rashid, M. Bernier, L. Pazdernick, R. Carpentier, Interaction of Zn^{2+} with the donor side of photosystem-II, Photosynth. Res. 30 (1991) 123–130.
[28] A. Rashid, E.L. Camm, A.K.M. Ekramoddoullah, Molecular mechanism of action of Pb^{2+} and Zn^{2+} on water oxidizing complex of photosystem II, FEBS Lett. 350 (1994) 296–298.
[29] C. Jegerschöld, J.B. Arellano, W.P. Schröder, P.J.M. van Kan, M. Baron, S. Styring, Copper(II) inhibition of electron-transfer through photosystem II studied by EPR spectroscopy, Biochemistry 34 (1995) 12747–12754.
[30] M.L. Ghirardi, T.W. Lutton, M. Seibert, Interactions between diphenylcarbazide, zinc, cobalt, and manganese on the oxidizing side of photosystem II, Biochemistry 35 (1996) 1820–1828.
[31] I. Yruela, G. Gatzen, R. Picorel, A.R. Holzwarth, Cu(II)-inhibitory effect on photosystem II from higher plants. A picosecond time-resolved fluorescence study, Biochemistry 35 (1996) 9469–9474.
[32] K. Burda, J. Kruk, G.H. Schmid, K. Strzalka, Inhibition of oxygen evolution in Photosystem II by Cu(II) ions is associated with oxidation of cytochrome *b*(559), Biochem. J. 371 (2003) 597–601.
[33] D.F. Ghanotakis, G.T. Babcock, C.F. Yocum, Structure of the oxygen-evolving complex of Photosystem II: calcium and lanthum compete for sites on the oxidizing side of Photosystem II which control the binding of water-soluble polypeptides and regulate the activity of the manganese complex, Biochim. Biophys. Acta 809 (1985) 173–180.
[34] D.A. Berthold, G.T. Babcock, C.F. Yocum, A highly resolved, oxygen-evolving photosystem II preparation from spinach thylakoid membranes—EPR and electron-transport properties, FEBS Lett. 134 (1981) 231–234.
[35] P.J. Smith, K.A. Åhrling, R.J. Pace, Nature of the S_2 state electron paramagnetic resonance signals from the oxygen-evolving complex of photosystem II—Q-band and oriented X-band studies, J. Chem. Soc., Faraday Trans. 89 (1993) 2863–2868.
[36] I.D. Arnon, Copper enzymes in isolated chloroplasts—polyphenoloxidase in beta-vulgaris, Plant Physiol. 24 (1949) 1–15.
[37] K.A. Campbell, W. Gregor, D.P. Pham, J.M. Peloquin, J.R. Debus, R.D. Britt, The 23 and 17 kDa extrinsic proteins of photosystem II modulate the magnetic properties of the S_1-state manganese cluster, Biochemistry 37 (1998) 5039–5045.
[38] F. Mamedov, H. Stefansson, P.-Å. Albertsson, S. Styring, Photosystem II in different parts of the thylakoid membrane: a functional comparison between different domains, Biochemistry 39 (2000) 10478–10486.
[39] I. Vass, S. Styring, pH-dependent charge equilibria between tyrosine-D and the S-states in photosystem 2. Estimation of relative midpoint redox potentials, Biochemistry 30 (1991) 830–839.
[40] S. Styring, A.W. Rutherford, Deactivation kinetics and temperature-dependence of the S-state transitions in the oxygen-evolving system of photosystem II measured by EPR spectroscopy, Biochim. Biophys. Acta 933 (1988) 378–387.
[41] G.W. Brudvig, J.L. Casey, K. Sauer, The effect of temperature on the formation and decay of the multiline EPR signal species associated with photosynthetic oxygen evolution, Biochim. Biophys. Acta 723 (1983) 366–371.
[42] A.-F. Miller, A.W. Brudvig, A guide to electron paramagnetic resonance spectroscopy of photosystem II membranes, Biochim. Biophys. Acta 1056 (1991) 1–18.
[43] G. Renger, H.-J. Eckert, A. Bergmann, J. Bernarding, B. Liu, A. Napiwotzki, F. Reifarth, H.J. Eichler, Fluorescence and spectroscopic studies of exciton trapping and electron-transfer in photosystem II of higher plants, Aust. J. Plant Physiol. 22 (1995) 167–181.
[44] F. Mamedov, E. Rintamäki, E.-M. Aro, B. Andersson, S. Styring, Influence of protein phosphorylation on the electron-transport properties of Photosystem II, Photosynth. Res. 74 (2002) 61–72.
[45] H.H. Robinson, A.R. Crofts, Kinetics of the oxidation reduction reactions of the photosystem II quinone acceptor complex, and the pathway for deactivation, FEBS Lett. 153 (1983) 221–226.
[46] P. Joliot, A. Joliot, B. Bouges, B. Barbieri, Studies of system-II photocenters by comparative measurements of luminescence, fluorescence and oxygen emission, Photochem. Photobiol. 14 (1971) 287–305.
[47] H.H. Robinson, A.R. Crofts, Kinetics of proton uptake and the oxidation–reduction reactions of the quinone acceptor complex of PS II from pea chloroplasts, in: C. Sybesma (Ed.), Adv. Photosynth. Res., vol. I, Martinus Nijhoff/Junk Publishers, The Hague, The Netherlands, 1984, pp. 477–484.
[48] W.F.J. Vermaas, A.W. Rutherford, EPR measurements on the effects of bicarbonate and triazine resistance on the acceptor side of photosystem II, FEBS Lett. 175 (1984) 243–248.
[49] A.W. Rutherford, J.-L. Zimmermann, A new EPR signal attributed to the primary plastosemiquinone acceptor in photosystem II, Biochim. Biophys. Acta 767 (1984) 168–175.
[50] V.V. Klimov, E. Dolan, E.R. Shaw, B. Ke, Interaction between the intermediary electron acceptor (pheophytin) and a possible plastoquinone–iron complex in photosystem II, Proc. Natl. Acad. Sci. U. S. A. 77 (1980) 7227–7231.
[51] Y. Sanakis, V. Petrouleas, B.A. Diner, Cyanide binding at the nonheme Fe^{2+} of the iron–quinone complex of photosystem II—at high concentrations, cyanide converts the Fe^{2+} from high (S=2) to low (S=0) spin, Biochemistry 33 (1994) 9922–9928.
[52] D.H. Stewart, G.W. Brudvig, Cytochrome *b*(559) of photosystem II, Biochim. Biophys. Acta 1367 (1998) 63–87.
[53] R. Gadjieva, F. Mamedov, G. Renger, S. Styring, Interconversion of low- and high-potential forms of cytochrome *b*(559) in tris-washed photosystem II membranes under aerobic and anaerobic conditions, Biochemistry 38 (1999) 10578–10584.
[54] O. Kaminskaya, J. Kurreck, K.-D. Irrgang, G. Renger, V.A. Shuvalov, Redox and spectral properties of cytochrome *b*(559) in different preparations of photosystem II, Biochemistry 38 (1999) 16223–16235.
[55] V.P. McNamara, K. Gounaris, Granal photosystem II complexes contain only the high redox potential from of cytochrome *b*-559 which is stabilized by the ligation of calcium, Biochim. Biophys. Acta 1231 (1995) 289–296.
[56] L.-E. Andreasson, I. Vass, S. Styring, Ca^{2+} depletion modifies the electron-transfer on both donor and acceptor sides in photosystem II from spinach, Biochim. Biophys. Acta 1230 (1995) 155–164.
[57] N. Lydakis-Simantiris, P. Dorlet, D.F. Ghanotakis, G.T. Babcock, Kinetic and spectroscopic properties of the Y_z center dot radical in Ca^{2+} and Cl^- -depleted photosystem II preparations, Biochemistry 37 (1998) 6427–6435.
[58] A. Boussac, P. Setif, A.W. Rutherford, Inhibition of tyrosine-Z photooxidation after formation of the S_3 state in Ca^{2+}-depleted and Cl^--depleted photosystem II, Biochemistry 31 (1992) 1224–1234.
[59] B. Svensson, C. Etchebest, P. Tuffery, P. van Kan, J. Smith, S. Styring, A model for the photosystem II reaction center core including the structure of the primary donor P-680, Biochemistry 35 (1996) 14486–14502.